

METHODS FOR MEASURING THE THERMODYNAMIC STABILITY OF MEMBRANE PROTEINS

Heedeok Hong,^{*,1} Nathan H. Joh,^{*,1} James U. Bowie,^{*}
and Lukas K. Tamm[†]

Contents

1. Introduction	214
2. Two Classes of Membrane Proteins	215
3. Methods for Measuring Transmembrane Domain Oligomer Stability	216
3.1. Analytical ultracentrifugation	217
3.2. Förster resonance energy transfer (FRET)	217
3.3. Disulfide cross-linking	218
3.4. Genetic assay systems (TOXCAT, POSSYCAT, and GALLEX)	218
4. Methods for Measuring Multipass α -helical Membrane Protein Stability	219
5. Methods to Study the Stability of β -barrel Membrane Proteins	222
5.1. SDS denaturation	223
5.2. Thermal denaturation	223
5.3. Solvent denaturation with urea or GdnHCl	224
6. A Few Salient Results on Forces that Stabilize Membrane Proteins	227
6.1. Van der Waals/packing interactions	227
6.2. Hydrogen-bonding interactions	228
6.3. Electrostatic interactions	228
6.4. Aromatic-aromatic interactions	228
6.5. Elastic lipid bilayer forces	229
7. Conclusion and Outlook	231
Acknowledgements	232
References	232

* Department of Chemistry and Biochemistry, UCLA-DOE Center for Genomics and Proteomics, Molecular Biology Institute, University of California, Los Angeles, California, USA

† Center for Membrane Biology and Department of Molecular Physiology and Biological Physics, University of Virginia Health System, Charlottesville, Virginia, USA

¹ These two authors contributed equally

Abstract

Learning how amino acid sequences define protein structure has been a major challenge for molecular biology since the first protein structures were determined in the 1960s. In contrast to the staggering progress with soluble proteins, investigations of membrane protein folding have long been hampered by the lack of high-resolution structures and the technical challenges associated with studying the folding process *in vitro*. In the past decade, however, there has been an explosion of new membrane protein structures and a slower but notable increase in efforts to study the factors that define these structures. Here we review the methods that have been used to evaluate the thermodynamic stability of membrane proteins and provide some salient examples of how the methods have been used to begin to understand the energetics of membrane protein folding.

1. INTRODUCTION

Exploring the molecular forces that govern the structure and function of proteins is essential to many of the fundamental pursuits of biochemistry, including structure prediction and design, understanding evolution, disease etiology, and drug design. Although integral membrane proteins are prevalent, comprising a third of all genomes, and carry out important biological functions, our understanding of the folding and stability determinants of this special class of proteins remains rudimentary.

A major challenge in the study of membrane protein folding is developing experimental systems that allow for controlled examination of the reaction. Folding studies require experimental conditions that drive unfolding but still enable complete refolding. In contrast to water-soluble proteins, folding studies in membrane proteins are complicated by the physical and chemical heterogeneity of the bilayer environment, which is matched by equally varied properties of the membrane protein. The physical forces that control folding also vary with the environment. It is therefore hard to find convenient experimental systems that can satisfy all the different constraints.

In this chapter we will discuss the *in vitro* experimental approaches that have been used to study the membrane protein folding thermodynamics. We will first introduce the two main classes of membrane proteins, namely α -helical and β -barrel proteins, and review the methods for thermodynamic characterization of folding and assembly for the two classes. We will not explicitly discuss studies of folding kinetics here, which have been covered in previous reviews (Booth and Curnow, 2006; Tamm *et al.*, 2001).

2. TWO CLASSES OF MEMBRANE PROTEINS

Two classes of membrane protein structures have been observed to date: α -helical membrane proteins, comprised of bundles of transmembrane helices, and β -barrel membrane proteins, built from membrane-spanning β strands (Fig. 8.1). The helical membrane proteins are generally found in the inner membranes of bacterial cells or the plasma membrane of eukaryotes, while the β -barrel class appears in the outer membrane of bacteria or mitochondria. Both architectures are able to satisfy the requirement for hydrophobic matching of the bilayer and the desire to satisfy hydrogen bonds, but they impose very different folding imperatives (Fig. 8.2).

In an α -helix, backbone hydrogen bonds can be satisfied locally so that an isolated hydrophobic helix can be effectively a stable domain within the bilayer (Engelman *et al.*, 1986). During helical membrane protein biogenesis, the translocon can shuttle individual helices or pairs of helices into the bilayer (Rapoport, 2007), enabling final folding to proceed after membrane insertion (Engelman *et al.*, 2003; Popot and Engelman, 1990). While we still do not have an experimental view of an unfolded membrane protein in a bilayer, the fact that individual secondary-structure elements can be stable suggests that it is reasonable to envision the unfolding of a helical membrane protein as a loss of tertiary structure in the bilayer, but not complete loss of stable helical transmembrane segments.

Unlike α -helices, individual β -strands of β -barrel membrane proteins are generally not stable in the hydrocarbon core of the bilayer. The

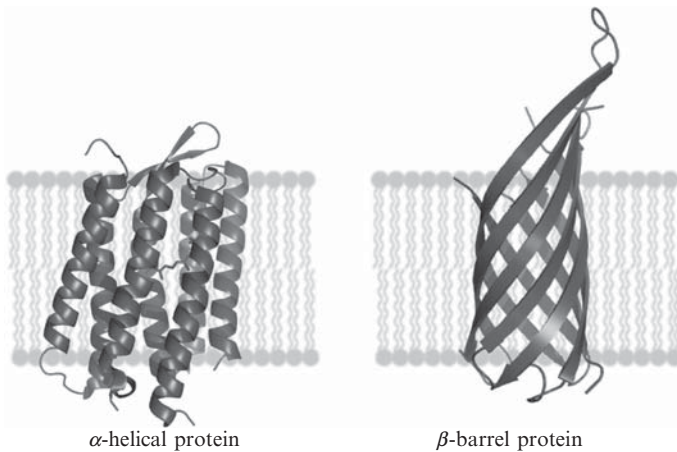


Figure 8.1 Structures of representative α -helical and β -barrel membrane proteins in a lipid bilayer. Left: bacteriorhodopsin (bR). Right: Transmembrane domain of outer membrane protein A (OmpA).

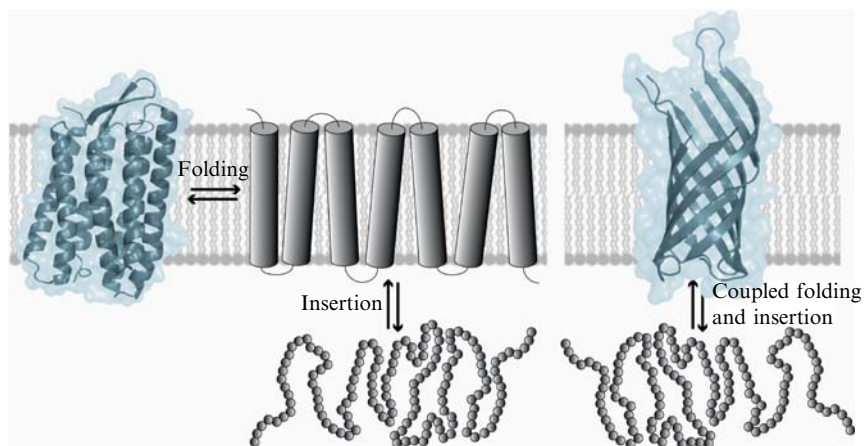


Figure 8.2 Thermodynamic folding pathways for α -helical and β -barrel membrane proteins. Left: Two-state model of α -helical membrane protein folding, adopted from Popot and Engelman (1990). Right: Coupled process of folding and insertion for β -barrel proteins.

backbone hydrogen bonds are not internally satisfied and the sequences tend to be relatively hydrophilic, with one face of the strand lining a polar pore and the other side facing the apolar core of the bilayer. Consequently the biogenesis of β -barrel membrane proteins is very different from the biogenesis of α -helical proteins, involving chaperones that ferry the protein to the membrane, and folding and insertion are highly coupled processes (Kleinschmidt and Tamm, 2002). Thus, unlike helical proteins, the unfolded protein is not likely to be inserted across the bilayer.

Because α -helical membrane protein folding and β -barrel membrane protein folding are different, they need to be studied in different ways. In this review we will discuss the techniques that have been applied to study membrane protein folding, their limitations and prospects for the future.

3. METHODS FOR MEASURING TRANSMEMBRANE DOMAIN OLIGOMER STABILITY

One way to access information about the energetics of molecular interactions in membrane proteins is by measuring dissociation constants of membrane protein subunits or isolated transmembrane (TM) helices. The assembly of individual TM helices also provides a model for the folding of larger helical membrane proteins from the unfolded, membrane-inserted form with intact transmembrane helices.

3.1. Analytical ultracentrifugation

After centrifugation of a protein to equilibrium, the concentration distribution in the cell is dependent on the effective mass of the protein (i.e., the mass of the molecule corrected for buoyancy). Because the equilibrium distribution does not depend on the shape of the molecule, it is an effective technique for obtaining molecular weights of well-behaved proteins. If the protein is an oligomer that dissociates in the concentration range of the centrifugation experiment, the concentration distribution will reflect the oligomerization equilibrium and the distribution can be fit to obtain dissociation constants.

In the case of membrane proteins, the situation is complicated because the sedimenting species is not the protein alone but the detergent-protein complex. This can be dealt with either by adjusting the solvent density (Choma *et al.*, 2000; Tanford *et al.*, 1974) or by judiciously choosing a detergent (Fleming *et al.*, 1997; Ludwig *et al.*, 1982). In an ideal case, the solvent density matches the detergent so that the detergent does not contribute to the effective mass of the protein in the centrifuge tube (Fleming, 2008).

Another significant difference between soluble and membrane proteins is the appropriate concentration units, and consequently, the standard state (Fleming, 2002). A membrane protein is generally confined to the volume defined by the micelle (Sehgal *et al.*, 2005), not the total solvent volume, so that increasing the detergent concentration decreases the effective concentration of the membrane protein, even if the bulk concentration has not been changed. Thus, the most appropriate concentration units are mole fraction units in the micelle phase.

3.2. Förster resonance energy transfer (FRET)

Förster resonance energy transfer (FRET) measurements have been used to analyze transmembrane helix dimerization energetics in various detergents. If the Förster distance for a selected donor and acceptor pair is greater than the interchromophore distance in the oligomer, an approximate average degree of association at a particular peptide-detergent ratio can be determined by measuring the variation in the fluorescence intensity of the donor attached to peptide as a function of the concentration of the acceptor while keeping the total peptide-detergent ratio constant (Adair and Engelman, 1994; Chung *et al.*, 1992; Gallivan and Dougherty, 1999; Reddy *et al.*, 1999). Then, by carrying out the measurements at different peptide-detergent ratios, dissociation constants can be determined.

Hristova and coworkers established that FRET methods could be applied to measuring free energies of helix-helix interactions in bilayers by demonstrating homogenization and equilibration of transmembrane

peptides integrated in either multilamellar or large unilamellar vesicles (You *et al.*, 2005). FRET measurements for different donor-acceptor ratios have to be made from individually prepared samples because homogenization by titration is hard to achieve in the vesicle system. The ability to measure dissociation constants in bilayers is a major advantage over equilibrium sedimentation that can use only detergent systems, but because there is a limited dilution range possible in vesicle systems, high-affinity interactions are inaccessible with this approach.

3.3. Disulfide cross-linking

DeGrado and coworkers introduced a disulfide cross-linking method to measure the free energy of transmembrane helix oligomerization in detergent micelles and, importantly, lipid vesicles (Cristian *et al.*, 2003). In this method, cysteines are introduced into the oligomerizing transmembrane peptide at positions where they can form disulfide bonds when they are in close proximity. If placed appropriately, disulfide formation is more favorable in the oligomer compared to the monomer. Thus, by measuring the fraction of disulfide formed as a function of reduction potential, it is possible to measure dimerization constants. Again, the ability to measure dissociation constants in bilayers is a major advantage, but high affinity interactions may be inaccessible because of the limited dilution range possible.

3.4. Genetic assay systems (TOXCAT, POSSYCAT, and GALLEX)

A number of genetic screens and selections have been developed to probe transmembrane helix oligomerization. Most of the methods tether a DNA binding domain that binds to DNA as a dimer to the TM domain. In this manner, DNA binding is coupled to TM domain oligomerization. By coupling gene expression to DNA binding, it is possible to assess TM domain oligomerization by monitoring gene expression. Langosch and coworkers developed the first system, using the transcriptional activator ToxR fused to the lacZ gene, which can be either used in a selection or readily screened using the well developed technology for detecting β -galactosidase activity (Gurezka and Langosch, 2001; Langosch *et al.*, 1996). In 1999, Russ and Engelman converted the approach into a genetic selection, called TOXCAT, in which the ToxR dimer regulates expression of chloramphenicol acetyl transferase (CAT), conferring chloramphenicol resistance (Russ and Engelman, 1999). Langosch and coworkers developed a similar system, called POSSYCAT, in which the CAT gene is in single copy on the chromosome (Gurezka and Langosch, 2001). Leeds and Beckwith developed a system in which the TM domain is fused to the N-terminal domain of λ -repressor, which can confer resistance to the lytic growth of phage λ (Leeds and Beckwith, 1998). Schneider and Engelman expanded the approach to

hetero-oligomers, employing a LexA DNA binding domain and named the assay GALLEX (Schneider and Engelman, 2003). Protein fragment complementation assays have also been developed to assess oligomerization in membranes (Remy and Michnick, 1999). Here two fragments of a protein that are inactive separately are fused to a membrane protein. Oligomerization brings the inactive fragments together where they can assemble and reconstitute activity. Thus, activity is coupled to oligomerization. To our knowledge, no genetic screens or selections have been implemented for antiparallel TM helix interactions, which would be a useful advance.

A major advantage of these genetic screens and selection systems is that a huge number of TM variants can be tested for their ability to oligomerize. Moreover, oligomerization is assessed in a natural membrane rather than a membrane mimetic environment. A disadvantage, however, is that free energies of association cannot be measured directly. Nevertheless, free energies are correlated with CAT expression in the TOXCAT system, which allows for approximate free energies to be inferred (Duong *et al.*, 2007; Russ and Engelman, 1999).

4. METHODS FOR MEASURING MULTIPASS α -HELICAL MEMBRANE PROTEIN STABILITY

Reversible folding, an essential requirement for making thermodynamic stability measurements, is not easily achieved for larger polytopic helical membrane proteins. Unfolding of helical membrane proteins induced by most methods, such as thermal and chemical approaches, is irreversible as reviewed by Stanley and Fleming (2008). Currently the only viable method for measuring complex α -helical membrane protein folding energetics is an SDS unfolding assay (Lau and Bowie, 1997).

Khorana and coworkers made the seminal observation that bacteriorhodopsin (bR) can be refolded from an SDS denatured state (London and Khorana, 1982). On the basis of this observation, Paula Booth pioneered studies of the mechanism of membrane protein folding by studying the kinetics of SDS unfolding and refolding (Booth *et al.*, 1996). Lau and Bowie (1997) developed a thermodynamic stability assay for the protein diacylglycerol kinase by monitoring unfolding as a function of SDS concentration. A similar assay was later used for measuring the stability of bR (Chen and Gouaux, 1999; Faham *et al.*, 2004) and the disulfide-bond thiooxidoreductase DsbB (Otzen, 2003), though in the latter case equilibrium constants were inferred by kinetic measurements (see also Curnow and Booth, 2007). The SDS unfolding assay is similar to urea and GuHCl denaturation of soluble proteins, except that a denaturing agent drives unfolding.

As with any method to monitor unfolding and refolding reactions, it is necessary to have an experimental probe that is sensitive to the conformational change. Methods that have been used include the far UV CD signal (Curnow and Booth, 2007; Lau and Bowie, 1997), the absorbance or fluorescence of Trp residues (Booth *et al.*, 1996; Otzen, 2003), and the retinal chromophore of bacteriorhodopsin (Booth *et al.*, 1996; Faham *et al.*, 2004).

Equilibrium unfolding with SDS is best illustrated by bR, as it is the best characterized and simplest system. A typical unfolding curve for bacteriorhodopsin monitored by retinal absorbance is shown in Fig. 8.3A. The unfolding curves for bR are fit under a number of assumptions that have varying levels of support. First, we assume that the system is in equilibrium throughout the experiment. This seems well justified by the finding that essentially the same curves are observed starting from the native state and adding SDS, or starting from the SDS denatured state and diluting the SDS (Lau and Bowie, 1997). Second, the unfolding reaction is assumed to be essentially two state, with minimal contributions from unfolding intermediates. The two-state assumption appears to be an excellent approximation because unfolding curves obtained by retinal absorbance and by far-UV circular dichroism, probes sensitive to very different structural parameters, show essentially the same unfolding curves (Curnow and Booth, 2007; Faham *et al.*, 2004) (see Fig. 8.3B). Third, we assume that the unfolding free energy is linear with SDS concentration using mole fraction units. As pointed out by Otzen and coworkers (Sehgal *et al.*, 2005), the best concentration units are micellar mole fraction, but we have used the bulk mole fraction. We originally applied this approach only because it is simple and appeared to fit the data well in the transition zones. More recently, measurements of folding and unfolding rates as a function of SDS concentration in the Booth lab also appear consistent with this simple analysis (Curnow and Booth, 2007). The theoretical justification remains unknown to our knowledge. As long as we keep extrapolations to a minimum, however, by calculating only unfolding free energies near the transition zones, large errors are unlikely. Fourth, we assume that the spectroscopic changes of the native state as a function of SDS concentration are linear. There is no justification for this assumption, but there is also no justification for a more complex model. We therefore apply the simplest model that fits the data. Applying these assumptions provides excellent fits to the unfolding curves and allows us to extract unfolding free energies in the transition zones (Fig. 8.3).

The nature of the unfolded state in SDS remains somewhat murky (Renthal, 2006). Neutron-scattering experiments with soluble proteins support a model where SDS micelles bind to the polypeptide chain, reminiscent of beads on a string (Ibel *et al.*, 1990). The polypeptide generally occupies the micelle surface, but presumably hydrophobic portions of the protein are more buried in the apolar micelle core. This model is consistent

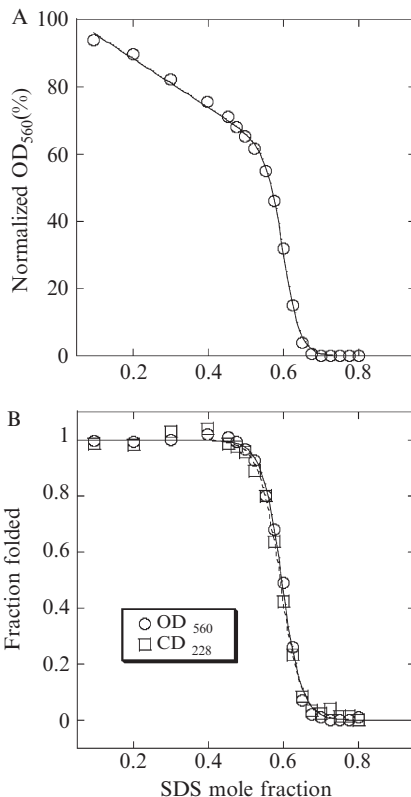


Figure 8.3 SDS unfolding of bR. (A) Unfolding of bR at a concentration of 0.1 mg/ml in bicelle composed of 15 mM 1,2-Dimyristoyl-*sn*-Glycero-3-Phosphocholine (DMPC), 6 mM 3-[(3-cholamidopropyl)dimethylammonio]-2-hydroxy-1-propanesulfonate (CHAPSO) and 10 mM sodium phosphate (pH 6.0) induced by titrating in 20% (w/v) SDS in the same bicelle mixture. Unfolding was monitored by detecting the absorption of the retinal chromophore at 560 nm. The fitted curve is obtained using the assumptions described in the text (*i.e.*, two-state folding, linear dependence of unfolding free energy with SDS concentration and linear dependence of the native state absorbance with SDS concentration). (B) Unfolding curves for bR generated by monitoring the retinal absorption at 560 nm (o) and far UV CD at 228 nm (□). The curves are essentially identical, consistent with a two-state assumption.

with the results from the Otzen group that the heat capacity decreases upon unfolding in SDS, which suggests additional shielding from solvent by SDS micelle binding (Sehgal and Otzen, 2006). It seems reasonable to suggest that, for membrane proteins, the hydrophobic TM helical segments can remain helical and somewhat buried in the micelle while the hydrophilic portions become associated with the polar head groups, but this is largely speculation.

How much structure remains within these putative micelle and polypeptide complexes? According to a straightforward interpretation of CD spectra, DsbB shows essentially no loss of helical content (Otzen, 2003), whereas bR and diacyl glycerolkinase lose about 40% and 15 % of helical content, respectively, upon unfolding in SDS (Faham *et al.*, 2004; Lau and Bowie, 1997). Renthall (2006) has pointed out that the helical content obtained from NMR structures in SDS are consistently higher than observed by CD measurements. He suggests that CD underestimates helical content in SDS, perhaps because of changes in peptide absorbance. On the other hand, nuclear Overhauser effects (NOEs) that are used to calculate nuclear magnetic resonance (NMR) structures are sometimes observed for transiently stabilized conformations and therefore may underestimate unraveled helices that may also be present in the ensemble. Moreover, the close correspondence of unfolding curves measured by far UV CD and other unfolding probes strongly suggest that CD changes reflect conformational changes rather than simply environmental effects on extinction coefficients (Faham *et al.*, 2004). The maintenance of considerable helical structure is an advantage of SDS unfolding because it somewhat resembles the presumed unfolded state in membranes in which transmembrane helix domains can remain folded (Popot and Engelman, 1990). It is an open question how much residual tertiary structure remains. Many membrane proteins, including bR, run normally in SDS-PAGE suggesting that the properties of the detergent and protein complexes are similar to soluble proteins, which appears inconsistent with a compact denatured state (Renthall, 2006). In our own unpublished hydrogen exchange results, we see an increase in water accessibility throughout bR, further suggesting a loss of folded structure. Moreover, an NMR structure of a two helix fragment of bR in SDS shows considerable maintenance of the TM helical structure, but no helix-helix interactions (Pervushin *et al.*, 1994). Nevertheless, it is clear that stable tertiary interactions can be maintained in SDS as various oligomers remain intact in SDS complexes. Thus, the possibility of unbroken tertiary interactions in SDS remains a caveat to the interpretation of these unfolding experiments (Renthall, 2006).

5. METHODS TO STUDY THE STABILITY OF β -BARREL MEMBRANE PROTEINS

Because of the completely different design principles of β -barrel membrane proteins, their unfolded reference state is different from that of α -helical membrane proteins. Therefore, both numerical values of measured stabilities as well as the methods to obtain these values are quite different. In favorable cases, the unfolded reference state of β -barrel membrane proteins is a completely denatured form that is no longer associated with lipids or other amphiphiles.

5.1. SDS denaturation

Beta-barrel membrane proteins are unusually resistant to denaturation by SDS due to their extensive cross-strand H-bonding network. Like many individual TM α -helices, unboiled samples of β -barrel membrane proteins do not unfold and show an anomalous migration behavior by SDS-PAGE. SDS molecules do not bind proportionally to the length of the polypeptide chain, which leads to faster or slower migration by SDS-PAGE than would be expected given their molecular mass. However, when membrane proteins of this class are boiled in SDS, they unfold completely, losing most of their secondary and tertiary structure. This phenomenon has been known since the early 1970s as heat modifiability of bacterial outer membrane proteins (Omps). The detailed mechanism of this denaturation is not well understood and different forms of even the same membrane protein can be modified up or down from the true molecular mass upon omission of the boiling step in SDS-PAGE. For example, folded full-length OmpA migrates at 30 kD, faster than unfolded 35 kD OmpA (Surrey and Jahning, 1992), whereas the folded TM domain of OmpA migrates at 21 kD, slower than the 19 kD unfolded form of this domain (Arora *et al.*, 2000). Complete heat modification requires and, therefore, is an indicator of the correct tertiary structure (i.e., closure of the β -barrel). Folding intermediates such as a membrane-surface adsorbed form and a partially inserted form, which have much of their native secondary structures already developed, migrate by unboiled SDS-PAGE as if they were completely denatured or at intermediate values (i.e., at 35 and 32 kD, respectively, for OmpA) (Kleinschmidt and Tamm, 1996).

Although SDS does not affect the folded structure of unboiled Omps, it does reduce their thermal stability. The thermal transition temperature (T_m) decreases approximately linearly over several decades as the mole-fraction of SDS is increased in a mixed SDS and nondenaturing detergent micelle system (Mogensen *et al.*, 2005).

5.2. Thermal denaturation

Measurements of thermal denaturation can provide Gibbs free energy (ΔG), enthalpy (ΔH), entropy (ΔS), and heat-capacity changes (ΔC_p) between the folded and unfolded states of proteins. While calorimetric and spectroscopic measurements have been employed to characterize these parameters for many soluble proteins (and to determine whether their unfolding is truly two state), reversible thermal denaturation of membrane proteins has so far not been achieved. However, there have been numerous studies using irreversible thermal denaturation to get more qualitative insights into the stability of β -barrel membrane proteins. A recent comparative study of a range of β -barrel membrane proteins of different sizes illustrates this nicely (Burgess *et al.*, 2008).

Some active transport systems of bacterial outer membranes have large 22-stranded β -barrels with an embedded plug domain. Thermal denaturation studies by differential scanning calorimetry (DSC) have demonstrated that the plug domain and the surrounding β -barrel are autonomous folding units. For example, the plug domain of the iron-siderophore transporter FhuA unfolded reversibly at 65 °C and the β -barrel denatured irreversibly at 74 °C (Bonhivers *et al.*, 2001). Substrate binding increased the reversible transition to 71 °C while the higher T_m transition remained unchanged. When the plug domain was deleted, the irreversible transition of the β -barrel decreased to 62 °C, indicating that the presence of the plug stabilized the barrel structure.

The autotransporter AIDA has a β -barrel TM domain (β_2) and a surface-located β_1 domain. Thermal denaturation in detergent micelles showed that the β_1 domain stabilizes the β_2 domain (Mogensen *et al.*, 2005). Similarly, the interfacial α -helix of the lipid A biosynthesis protein PagP stabilized its β -barrel TM domain (Huysmans *et al.*, 2007).

Subunit interactions between monomers of trimeric porins may also be studied by thermal denaturation. For example, mutations breaking inter-subunit salt bridges have been shown to decrease the trimer-monomer T_m of OmpF from 72 to about 50 °C and ΔH_{cal} from 430 to about 280 kcal/mol (Phale *et al.*, 1998). These examples show that even in the absence of full thermodynamic descriptions, thermal denaturation studies are quite useful for analyzing domain and subunit interactions in β -barrel membrane proteins.

5.3. Solvent denaturation with urea or GdnHCl

In favorable cases, reversible refolding from a completely denatured state in solution to the native state in lipid bilayers can be achieved with β -barrel membrane proteins. This was first demonstrated for OmpA in lipid bilayers of different lipid compositions (Hong *et al.*, 2004). In these experiments, completely solubilized unfolded protein in 8 M urea (or 6 M GdnHCl) in the absence of detergent was refolded in the lipid bilayer of interest. Besides the aforementioned SDS-PAGE assay with unboiled samples, fluorescence spectroscopy, limited proteolysis, and single channel conductance measurements in planar lipid bilayers were used to ascertain quantitative conversion to the native structure (Arora *et al.*, 2000).

Unfolding of OmpA was monitored by SDS-PAGE, Trp fluorescence, and CD spectroscopy at different concentrations of denaturant. A plot of unfolded fraction versus denaturant concentration showed sigmoidal curves with fairly sharp transitions (Fig. 8.4). To prove reversibility the reverse experiment was also performed: unfolded protein was incubated with lipid bilayers at increasing amounts of denaturant and the unfolded fraction was determined. The unfolding and refolding curves were practically identical

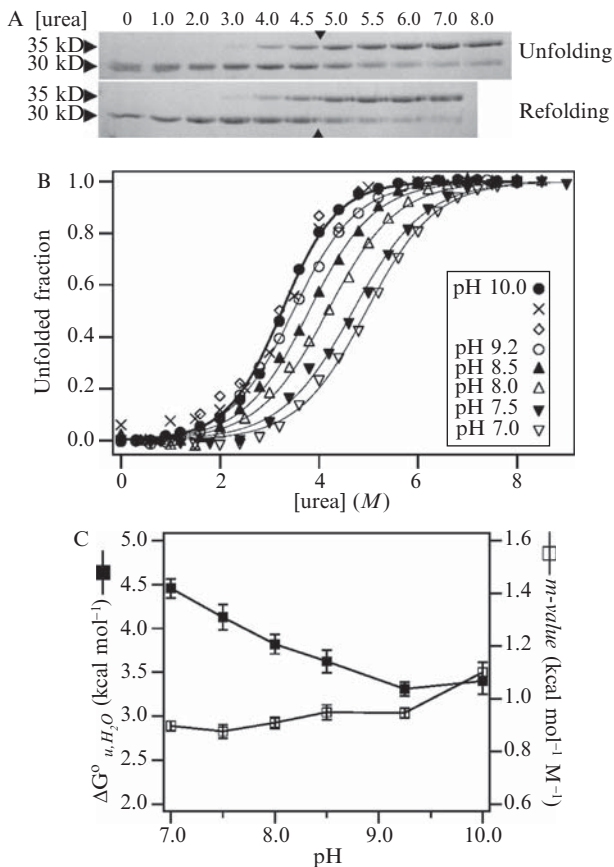


Figure 8.4 Two-state equilibrium folding of OmpA in bilayers at different values of pH. (A) Equilibrium unfolding (upper gel) and refolding (lower gel) of OmpA in $C_{16:0}C_{18:1}PC$: $C_{16:0}C_{18:1}PG$ lipid bilayers (92.5:7.5) measured by SDS-PAGE of unboiled samples. The approximate midpoints of transition are indicated by arrows. The unfolding and refolding reactions were incubated overnight in 10 mM HEPES buffer (pH 7.5) containing 2 mM EDTA. The protein concentration and the lipid-to-protein ratio were 5.6 μM and 800, respectively. (B) pH-dependent equilibrium unfolding measured by Trp fluorescence. The protein concentration and the lipid-to-protein ratio were 1.4 μM and 800, respectively. The unfolding curves at pH 10.0 obtained by Trp fluorescence (filled circles), far-UV circular dichroism (crosses), and the SDS PAGE shift assay (open diamonds), which are measures of lipid binding, secondary structure, and tertiary structure, respectively, superimpose in equilibrium measurements although they are not all synchronized in kinetic experiments. (C) Free energy of unfolding $\Delta G_{u,H_2O}^\circ$ of OmpA in $C_{16:0}C_{18:1}PC$: $C_{16:0}C_{18:1}PG$ bilayers as a function of pH. The free energies and m -values were obtained from best fits of the data of panel B to the two-state model described by Eqs. (8.3) and (8.4).

(see also Fig. 8.4A). A small amount (typically 5% to 10 mol %) of the negatively charged lipid POPG was included in the bilayer and the experiments were performed under basic and low salt conditions ($\text{pH} > 7.5$, $[\text{NaCl}] < 30 \text{ mM}$). This ensured that the denatured state of the protein became completely dissociated from the membrane surface by electrostatic repulsion (the calculated pI of OmpA is 5.6).

Figures 8.4B and 8.4C show the pH dependence of the equilibrium folding of OmpA in lipid bilayers. The fact that the unfolding and refolding curves monitored by Trp fluorescence, far-UV CD and SDS-PAGE were reversible and exactly superimposed (shown for pH 10 only, bold curve in Fig. 8.4B) strongly suggests that the transition is in two-state equilibrium because the three detection methods were previously shown to report on different kinetic phases of the folding pathway of OmpA (Kleinschmidt and Tamm, 2002).

For a two-state equilibrium transition the free energy of unfolding as a function of denaturant is defined as follows:

$$\Delta G_u^\circ = -RT \ln K_u = -RT \ln ([\text{unfolded}]/[\text{folded}]) \quad (8.1)$$

Linear extrapolation of the free energy to 0 M urea allows one to calculate the free energy of unfolding in water, $\Delta G_{u,\text{H}_2\text{O}}^\circ$, and the proportionality constant m (Greene and Pace, 1974).

$$\Delta G_{u,\text{H}_2\text{O}}^\circ = \Delta G_u^\circ + m [\text{urea}] \quad (8.2)$$

In practice, the equilibrium unfolding curve monitored by the average emission wavelength $\langle \lambda \rangle$, defined as $\langle \lambda \rangle = \Sigma(F_i \lambda_i) / \Sigma(F_i)$, where λ_i and F_i are the wavelength and the corresponding fluorescence intensity at the i th measuring step in the spectrum, respectively, is fitted to the following form of the two-state model (Mann *et al.*, 1993).

$$\langle \lambda \rangle = \frac{\langle \lambda \rangle_F + \langle \lambda \rangle_U \frac{1}{Q_R} \exp[m([\text{denaturant}] - C_m)/RT]}{1 + \frac{1}{Q_R} \exp[m([\text{denaturant}] - C_m)/RT]} \quad (8.3)$$

Here, $\langle \lambda \rangle_F$ and $\langle \lambda \rangle_U$ are the average emission wavelengths of the folded and unfolded states, respectively, determined from linear extrapolations of the two plateau values of the transition curve to 0 M urea. C_m is the urea concentration where folded and unfolded fractions are equal. Q_R is the relative ratio of the total fluorescence intensity of the native state to that of the unfolded state and is needed for normalization when one uses $\langle \lambda \rangle$'s to represent species concentrations. The free energy of unfolding is obtained from the fitted values of C_m and m .

$$\Delta G_{u,H_2O}^{\circ} = mC_m \quad (8.4)$$

When the data of Fig. 8.4 were analyzed with this model, it was found that the stability ($-\Delta G_{u,H_2O}^{\circ}$) of OmpA decreased from -4.5 kcal/mol to -3.4 kcal/mol when the pH increased from 7 to 10 (Fig. 8.4C). The significance of the m -value, which did not vary much with pH, has been debated extensively in the protein folding literature. For soluble proteins, it is often thought that this value, which is also a measure of the cooperativity of the system, is related to the residue hydrophobic surface area that becomes exposed to solvent upon denaturation. What this means exactly for membrane proteins is not so clear at this time.

The rather small stabilities of OmpA (-3.4 kcal/mol at pH 10 reported by Hong and Tamm (2004) and -9.3 kcal/mol for a different bilayer system reported by Hong *et al.* (2007) are of the same order of magnitude as for water-soluble proteins of similar size. This might be surprising at first sight when one considers the extreme heat resistance of this and other β -barrel membrane proteins. However, if one simply calculates the free energy of transfer of all residues that are transferred into the lipid bilayer with the augmented Wimley-White hydrophobicity scale (Jayasinghe *et al.*, 2001), one finds that the net ΔG° amounts to only about -1 kcal/mol. Cross-strand hydrogen bonding in the membrane likely drives the reaction further but is counteracted by favorable hydrogen bonding with water in the denatured state in solution. Obviously, and as is true for soluble protein folding, the energetics of membrane protein folding are driven by a delicate balance between large numbers of much larger attractive and repulsive forces.

6. A FEW SALIENT RESULTS ON FORCES THAT STABILIZE MEMBRANE PROTEINS

Although this is a review on thermodynamic methods to study membrane protein folding, we include a few salient results to better illustrate the usefulness of these methods. In this section we intentionally cherry-pick a few examples and do not intend to provide a comprehensive review on this rather broad topic.

6.1. Van der Waals/packing interactions

Van der Waals packing is clearly an important factor stabilizing helical membrane proteins. Indeed, TM helices with no polar side chains can form stable oligomers (Popot and Engelman, 2000). Intimate packing provided by the GxxxG (Russ and Engelman, 1999), glycine zipper (Kim

et al., 2004; Wu *et al.*, 2005), and leucine zipper motifs (Gurezka *et al.*, 1999) provides the necessary structural complementarity for packing of TM helices (MacKenzie *et al.*, 1997). Faham *et al.* (2004) found very similar energetic contributions of both polar and nonpolar side chains to the stability of bacteriorhodopsin. As nonpolar side chains constitute the vast majority of residues in the membrane, the results suggest that packing forces dominate.

6.2. Hydrogen-bonding interactions

It has been widely assumed that hydrogen bonds in membrane proteins should be strong because of the lack of competition from water and the low dielectric environment inside the bilayer, which should strengthen electrostatic interactions. This idea is supported by the increased hydrogen-bond strength seen for model compounds in apolar solvents relative to water (Klotz and Franzen, 1962). Most hydrogen-bonding interactions between side chains occur within a protein environment, however, not a membrane, so that an apolar solvent may not be a good model for these bonds. Indeed, the elimination of hydrogen bonds between oligomer subunits usually leads to quite modest changes in stability (Duong *et al.*, 2007; Gratkowski *et al.*, 2001; Hristova, 2008; Li *et al.*, 2006; Stanley and Fleming, 2007), although some contribute more than 1 kcal/mol. Eight hydrogen-bonded side-chain interactions in bacteriorhodopsin were recently evaluated by double mutant-cycle analysis and found to contribute only -0.6 kcal/mol on an average (Joh *et al.*, 2008). Thus, hydrogen bonds between side chains appear to be a net stabilizing force in membrane proteins, albeit not a dominant one.

6.3. Electrostatic interactions

OmpA contains a cluster of charged residues consisting of Glu52, Arg138, Glu128 and Lys82 surrounded by aromatic residues Tyr8, Phe40 and Tyr94 in the center of the β -barrel (Fig. 8.5). A salt bridge between Glu52 and Arg138 on opposite walls of the barrel interior forms a complete barrier or gate for ionic conduction through this channel protein. Using double mutant-cycle analysis combined with urea-induced equilibrium unfolding, Hong *et al.* (2006) determined the strength of this salt bridge to be -5.6 kcal/mol. This is as strong as the strongest salt bridges observed deeply buried inside soluble proteins. Other pairwise electrostatic interaction energies in this charge tetrad were found to range from -0.6 to -3.5 kcal/mol (Fig. 8.5).

6.4. Aromatic-aromatic interactions

Statistical analysis of membrane proteins of known structure and genomic sequence searches for identifying transmembrane segments of α -helical and β -barrel membrane proteins show that aromatic residues are dramatically

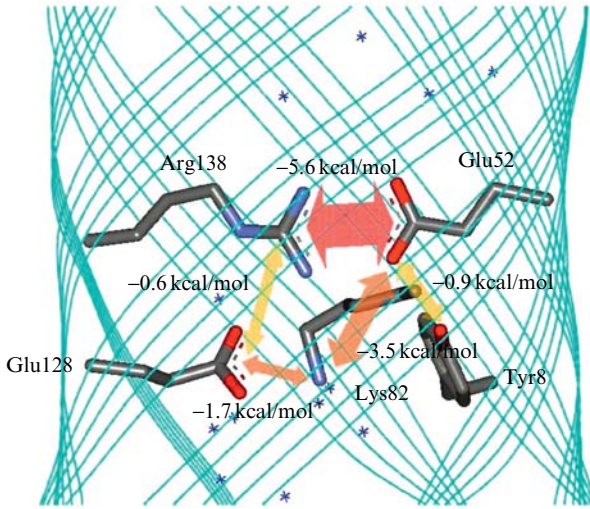


Figure 8.5 Electrostatic interactions in gating region of OmpA. The interaction energies were determined from double mutant-cycle analysis (used with permission from [Hong *et al.*, 2006](#)).

enriched in regions of the protein that contact the membrane–water interface ([Adamian *et al.*, 2005](#); [Granseth *et al.*, 2005](#); [Landolt–Marticorena *et al.*, 1993](#); [Senes *et al.*, 2007](#); [Ulmschneider *et al.*, 2005](#); [Wimley, 2002](#)). This prevalence is recapitulated in partition experiments of aromatic residue-containing model peptides to the membrane interface ([Wimley and White, 1996](#)). The first thermodynamic measurements of aromatic side-chain contribution to membrane protein stability in bilayers of a bona fide integral membrane protein were performed with OmpA ([Hong *et al.*, 2007](#)). It was found that isolated Trp, Tyr, and Phe residues (with no neighboring aromatic residues within a 7 Å radius) contribute on average -2.0 , -2.6 , and -1.0 kcal/mol, respectively, to the stability of this membrane protein. An unexpected new discovery of this study was that pairs of aromatic residues within a 7 Å range contribute even more stability than they would individually. Pairwise interaction energies in the range from -0.7 to -1.4 kcal/mol were measured between aromatic residues of OmpA that reside in the lipid interface of OmpA. This is in the same range known for similar interactions in water soluble proteins ([Burley and Petsko, 1985](#); [Serrano *et al.*, 1991](#)).

6.5. Elastic lipid bilayer forces

The molecular packing of lipids in a fluid bilayer is maintained by a combination of several forces: headgroup repulsion in the polar region, surface tension in the polar–nonpolar interface, and chain repulsion in the core region

(Marsh, 2007). These forces create a lateral pressure profile along the membrane normal, which cannot be directly measured but has been theoretically calculated (Cantor, 1999). It is not surprising that this pressure profile modulates the function of many integral membrane proteins, including receptors, ion channels, and enzymes (Botelho *et al.*, 2006; Perozo, 2002; Rostovtseva *et al.*, 2006). Internal membrane pressures also modulate the thermodynamic stability of membrane proteins, as was demonstrated with OmpA (Hong and Tamm, 2004). Including short-chain lipids in a reference bilayer increases the pressure in the interface region and including long-chain lipids with small headgroups and/or increasing the number of double bonds in the acyl chains increases the pressure in the core region of the bilayer. When the bilayer thickness was increased the stability of OmpA increased by -0.34 kcal/mol per Å of additional bilayer thickness (Fig. 8.6). With the known circumference of the OmpA barrel this converts to -4 cal/mol per Å² of increased hydrophobic contact area (i.e., about 20% of what would be expected from the hydrophobic effect) (Tanford, 1979). Another approximately -1.4 kcal/mol per Å bilayer thickness is probably counteracted by an elastic lipid deformation energy due to a hydrophobic mismatch between the hydrophobic thickness of the protein and the equilibrium bilayer thickness in the absence of the protein. Because it can be estimated that about 25 lipids form the first shell of boundary lipid around OmpA, the energy for stretching or compressing a lipid molecule should be around 50–60 cal/mol/Å if the first lipid shell absorbed all mismatch deformation. In reality this energy would probably be distributed into further layers of lipid around the protein, decaying quite rapidly from the perimeter of the protein.

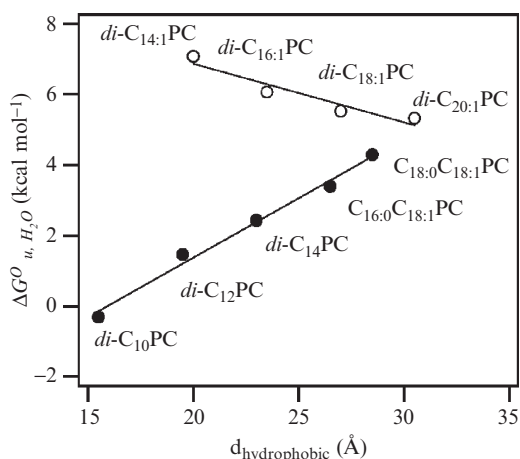


Figure 8.6 The stability of OmpA depends on bilayer thickness and curvature strain. Dependence of $\Delta G^{\circ}_{u, H_2O}$ on the hydrophobic thickness of PC bilayers with saturated and monounsaturated acyl chains (filled circles) and *cis*-double-unsaturated acyl chains (open circles).

7. CONCLUSION AND OUTLOOK

Although the biogenic pathways of inserting membrane proteins into the bilayers of biological membranes are guided by chaperones and specific insertion machineries *in vivo*, it is fundamentally important to understand the forces that ultimately determine the final structures that membrane proteins adopt in lipid bilayers. Understanding these forces not only is of academic interest but also can guide future design of membrane proteins with altered functions and, from a practical standpoint of structural biologists, with better properties for forming two- and three-dimensional crystals or improved stabilities for NMR studies.

With the advent of methods for evaluating the energetic effects of mutations on membrane protein thermodynamic stability, we have started to develop a quantitative, experiment-based picture of how protein sequences drive the formation of membrane protein structure. This is important because the elementary interactions that determine the folds of membrane proteins cannot be derived *a priori* from the vast existing knowledge of such forces in the soluble-protein-folding field. Some forces are similar, but others are very different in the complex milieu of lipid bilayers. Moreover, even for those elementary interactions that are similar, different sets of forces likely dominate the determination of the ultimate fold of membrane and soluble proteins.

A challenge in this field has been to find appropriate conditions to generate unfolded states that refold reversibly into native states. As illustrated in this chapter, substantial progress has been made in this regard in the last few years for both α -helical and β -barrel membrane proteins. Despite this progress a lot of work remains. The unfolded states, especially for α -helical membrane proteins are still not very well defined. Because the denatured states of helical membrane proteins harbor significant amounts of secondary structures associated with SDS or other denaturing detergents, it is probably wise to directly compare only measurements done on the same protein with each other rather than try to make comparisons between different α -helical membrane proteins. However, the double mutant-cycle approaches that have been developed for both α -helical and β -sheet membrane proteins elegantly circumvent this problem (Hong *et al.*, 2007; Hong *et al.*, 2006; Joh *et al.*, 2008). It does not matter what the denatured state really is as long as the effects of the mutations are independent.

With β -barrel membrane proteins we are also beginning to understand the complexities that the lipid bilayer imparts on the folding reaction. Not surprisingly, the stability of these and probably also α -helical proteins depends on bilayer properties in a major way. Bilayer thickness, intrinsic curvature, specific chemistries of headgroup structures, and so on affect the

folding of membrane proteins. Biological membranes contain thousands of different lipid species. So, what is the best lipid background for folding studies of these proteins? The answer to this question is not clear at this point, and it may be that different lipid mixtures will have to be defined as appropriate reference states for membrane proteins that reside in different membranes in the cell.

Although TM helix interactions can be studied in bilayers, there are still no methods for studying the folding of polytopic membrane proteins within a membrane. More needs to be done to explore the contribution of bilayer properties and how the energetics of molecular interactions vary with bilayer depth. The development of methods for unfolding and folding helical proteins in bilayers should be a major goal for the field.

The tools for studying the folding thermodynamics discussed in this chapter have enabled our first forays into the energetics of membrane protein folding. However, there are vast new territories that will need to be explored in this field for decades to come. Membrane proteins have to catch up with 40 years of tremendous activity and accumulated knowledge on the folding and energetics of soluble proteins. No doubt time will add new tools and new, increasingly sophisticated insights. The field is still in its infancy, and we look forward to substantial growth as well as practical applications as it matures.

ACKNOWLEDGEMENTS

Supported by grants GM063919 and GM081783 (J.U.B.) and GM051329 (L.K.T.) from the National Institutes of Health.

REFERENCES

- Adair, B., and Engelman, D. (1994). Glycophorin A helical transmembrane domains dimerize in phospholipid bilayers: A resonance energy transfer study. *Biochemistry* **33**, 5539–5544.
- Adamian, L., Nanda, V., DeGrado, W. F., and Liang, J. (2005). Empirical lipid propensities of amino acid residues in multispan alpha helical membrane proteins. *Proteins* **59**, 496–509.
- Arora, A., Rinehart, D., Szabo, G., and Tamm, L. K. (2000). Refolded outer membrane protein A of *Escherichia coli* forms ion channels with two conductance states in planar lipid bilayers. *J. Biol. Chem.* **275**, 1594–1600.
- Bonhivers, M., Desmadril, M., Moeck, G. S., Boulanger, P., Colomer-Pallas, A., and Letellier, L. (2001). Stability studies of FhuA, a two-domain outer membrane protein from *Escherichia coli*. *Biochemistry* **40**, 2606–2613.
- Booth, P., Farooq, A., and Flitsch, S. (1996). Retinal binding during folding and assembly of the membrane protein bacteriorhodopsin. *Biochemistry* **35**, 5902–5909.
- Booth, P. J., and Curnow, P. (2006). Membrane proteins shape up: Understanding in vitro folding. *Curr. Opin. Struct. Biol.* **16**, 480–488. Epub 2006 July 3.

- Botelho, A. V., Huber, T., Sakmar, T. P., and Brown, M. F. (2006). Curvature and hydrophobic forces drive oligomerization and modulate activity of rhodopsin in membranes. *Biophys. J.* **91**, 4464–4477.
- Burgess, N. K., Dao, T. P., Stanley, A. M., and Fleming, K. G. (2008). Beta-barrel proteins that reside in the *E. coli* outer membrane *in vivo* demonstrate varied folding behavior *in vitro*. *J. Biol. Chem.* **283**, 26748–26758.
- Burley, S. K., and Petsko, G. A. (1985). Aromatic-aromatic interaction: A mechanism of protein structure stabilization. *Science* **229**, 23–28.
- Cantor, R. S. (1999). Lipid composition and the lateral pressure profile in bilayers. *Biophys. J.* **76**, 2625–2639.
- Chen, G. Q., and Gouaux, E. (1999). Probing the folding and unfolding of wild-type and mutant forms of bacteriorhodopsin in micellar solutions: Evaluation of reversible unfolding conditions. *Biochemistry* **38**, 15380–15387.
- Choma, C., Gratkowski, H., Lear, J. D., and DeGrado, W. F. (2000). Asparagine-mediated self-association of a model transmembrane helix. *Nat. Struct. Biol.* **7**, 161–166.
- Chung, L., Lear, J., and DeGrado, W. (1992). Fluorescence studies of the secondary structure and orientation of a model ion channel peptide in phospholipid vesicles. *Biochemistry* **31**, 6608–6616.
- Cristian, L., Lear, J. D., and DeGrado, W. F. (2003). Use of thiol-disulfide equilibria to measure the energetics of assembly of transmembrane helices in phospholipid bilayers. *Proc. Natl. Acad. Sci. USA* **100**, 14772–14777.
- Curnow, P., and Booth, P. (2007). Combined kinetic and thermodynamic analysis of alpha-helical membrane protein unfolding. *Proc. Natl. Acad. Sci. USA* **104**, 18970–18975.
- Duong, M. T., Jaszewski, T. M., Fleming, K. G., and MacKenzie, K. R. (2007). Changes in apparent free energy of helix-helix dimerization in a biological membrane due to point mutations. *J. Mol. Biol.* **371**, 422–434.
- Engelman, D., Chen, Y., Chin, C., Curran, A., Dixon, A., Dupuy, A., Lee, A., Lehnert, U., Matthews, E., Reshetnyak, Y., Senes, A., and Popot, J. (2003). Membrane protein folding: Beyond the two stage model. *FEBS Lett.* **555**, 122–125.
- Engelman, D. M., Steitz, T. A., and Goldman, A. (1986). Identifying nonpolar transbilayer helices in amino acid sequences of membrane proteins. *Annu. Rev. Biophys. Chem.* **15**, 321–353.
- Faham, S., Yang, D., Bare, E., Yohannan, S., Whitelegge, J., and Bowie, J. (2004). Side-chain contributions to membrane protein structure and stability. *J. Mol. Biol.* **335**, 297–305.
- Fleming, K., Ackerman, A., and Engelman, D. (1997). The effect of point mutations on the free energy of transmembrane alpha-helix dimerization. *J. Mol. Biol.* **272**, 266–275.
- Fleming, K. G. (2002). Standardizing the free energy change of transmembrane helix-helix interactions. *J. Mol. Biol.* **323**, 563–571.
- Fleming, K. G. (2008). Determination of membrane protein molecular weight using sedimentation equilibrium analytical ultracentrifugation. *Curr. Protoc. Protein Sci.* Unit 7.12.1–7.12.13.
- Gallivan, J. P., and Dougherty, D. A. (1999). Cation-pi interactions in structural biology. *Proc. Natl. Acad. Sci. USA* **96**, 9459–9464.
- Granseth, E., von Heijne, G., and Elofsson, A. (2005). A study of the membrane-water interface region of membrane proteins. *J. Mol. Biol.* **346**, 377–385.
- Gratkowski, H., Lear, J., and DeGrado, W. (2001). Polar side chains drive the association of model transmembrane peptides. *Proc. Natl. Acad. Sci. USA* **98**, 880–885.
- Greene, R. F. Jr., and Pace, C. N. (1974). Urea and guanidine hydrochloride denaturation of ribonuclease, lysozyme, alpha-chymotrypsin, and beta-lactoglobulin. *J. Biol. Chem.* **249**, 5388–5393.

- Gurezka, R., Laage, R., Brosig, B., and Langosch, D. (1999). A heptad motif of leucine residues found in membrane proteins can drive self-assembly of artificial transmembrane segments. *J. Biol. Chem.* **274**, 9265–9270.
- Gurezka, R., and Langosch, D. (2001). *In vitro* selection of membrane-spanning leucine zipper protein-protein interaction motifs using POSSYCCAT. *J. Biol. Chem.* **276**, 45580–45587.
- Hong, H., Park, S., Jimenez, R. H., Rinehart, D., and Tamm, L. K. (2007). Role of aromatic side chains in the folding and thermodynamic stability of integral membrane proteins. *J. Am. Chem. Soc.* **129**, 8320–8327.
- Hong, H., Szabo, G., and Tamm, L. K. (2006). Electrostatic couplings in OmpA ion-channel gating suggest a mechanism for pore opening. *Nat. Chem. Biol.* **2**, 627–635.
- Hong, H., and Tamm, L. K. (2004). Elastic coupling of integral membrane protein stability to lipid bilayer forces. *Proc. Natl. Acad. Sci. USA* **101**, 4065–4070.
- Hristova, K. (2008). Pathogenic activation of receptor dimers in mammalian membranes. In “FASEB summer research conferences; Molecular biophysics of cellular membranes” (J. U. Bowie, ed.), Saxtons River, Vermont.
- Huysmans, G. H., Radford, S. E., Brockwell, D. J., and Baldwin, S. A. (2007). The N-terminal helix is a post-assembly clamp in the bacterial outer membrane protein PagP. *J. Mol. Biol.* **373**, 529–540.
- Ibel, K., May, R. P., Kirschner, K., Szadkowski, H., Mascher, E., and Lundahl, P. (1990). Protein-decorated micelle structure of sodium-dodecyl-sulfate—protein complexes as determined by neutron scattering. *Eur. J. Biochem.* **190**, 311–318.
- Jayasinghe, S., Hristova, K., and White, S. H. (2001). Energetics, stability, and prediction of transmembrane helices. *J. Mol. Biol.* **312**, 927–934.
- Joh, N. H., Min, A., Faham, S., Whitelegge, J. P., Yang, D., Woods, V. L., and Bowie, J. U. (2008). Modest stabilization by most hydrogen-bonded side-chain interactions in membrane proteins. *Nature* **453**, 1266–1270.
- Kim, S., Chamberlain, A., and Bowie, J. (2004). Membrane channel structure of *Helicobacter pylori* vacuolating toxin: Role of multiple GXXXG motifs in cylindrical channels. *Proc. Natl. Acad. Sci. USA* **101**, 5988–5991.
- Kleinschmidt, J. H., and Tamm, L. K. (1996). Folding intermediates of a beta-barrel membrane protein: Kinetic evidence for a multi-step membrane insertion mechanism. *Biochemistry* **35**, 12993–13000.
- Kleinschmidt, J. H., and Tamm, L. K. (2002). Secondary and tertiary structure formation of the beta-barrel membrane protein OmpA is synchronized and depends on membrane thickness. *J. Mol. Biol.* **324**, 319–330.
- Klotz, I. M., and Franzen, J. S. (1962). Hydrogen bonds between model peptide groups in solution. *J. Am. Chem. Soc.* **84**, 3461–3466.
- Landolt-Marticorena, C., Williams, K. A., Deber, C. M., and Reithmeier, R. A. (1993). Non-random distribution of amino acids in the transmembrane segments of human type I single span membrane proteins. *J. Mol. Biol.* **229**, 602–608.
- Langosch, D., Brosig, B., Kolmar, H., and Fritz, H. J. (1996). Dimerisation of the glycoporphin A transmembrane segment in membranes probed with the ToxR transcription activator. *J. Mol. Biol.* **263**, 525–530.
- Lau, F., and Bowie, J. (1997). A method for assessing the stability of a membrane protein. *Biochemistry* **36**, 5884–5892.
- Leeds, J. A., and Beckwith, J. (1998). Lambda repressor N-terminal DNA-binding domain as an assay for protein transmembrane segment interactions *in vivo*. *J. Mol. Biol.* **280**, 799–810.
- Li, E., You, M., and Hristova, K. (2006). FGFR3 dimer stabilization due to a single amino acid pathogenic mutation. *J. Mol. Biol.* **356**, 600–612.
- London, E., and Khorana, H. (1982). Denaturation and renaturation of bacteriorhodopsin in detergents and lipid-detergent mixtures. *J. Biol. Chem.* **257**, 7003–7011.

- Ludwig, B., Grabo, M., Gregor, I., Lustig, A., Regenass, M., and Rosenbusch, J. P. (1982). Solubilized cytochrome c oxidase from *Paracoccus denitrificans* is a monomer. *J. Biol. Chem.* **257**, 5576–5578.
- MacKenzie, K., Prestegard, J., and Engelman, D. (1997). A transmembrane helix dimer: Structure and implications. *Science* **276**, 131–133.
- Mann, C. J., Royer, C. A., and Matthews, C. R. (1993). Tryptophan replacements in the trp aporepressor from *Escherichia coli*: Probing the equilibrium and kinetic folding models. *Protein Sci.* **2**, 1853–1861.
- Marsh, D. (2007). Lateral pressure profile, spontaneous curvature frustration, and the incorporation and conformation of proteins in membranes. *Biophys. J.* **93**, 3884–3899.
- Mogensen, J. E., Kleinschmidt, J. H., Schmidt, M. A., and Otzen, D. E. (2005). Misfolding of a bacterial autotransporter. *Protein Sci.* **14**, 2814–2827.
- Otzen, D. (2003). Folding of DsbB in mixed micelles: A kinetic analysis of the stability of a bacterial membrane protein. *J. Mol. Biol.* **330**, 641–649.
- Perozo, E., Cortes, D. M., Sompornpisut, P., Kloda, A., and Martinac, B. (2002). Open channel structure of MscL and the gating mechanism of mechanosensitive channels. *Nature* **418**, 942–948.
- Pervushin, K. V., Orekhov, V., Popov, A. I., Musina, L., and Arseniev, A. S. (1994). Three-dimensional structure of (1–71)bacterioopsin solubilized in methanol/chloroform and SDS micelles determined by ¹⁵N-1H heteronuclear NMR spectroscopy. *Eur. J. Biochem.* **219**, 571–583.
- Phale, P. S., Philippsen, A., Kiefhaber, T., Koebnik, R., Phale, V. P., Schirmer, T., and Rosenbusch, J. P. (1998). Stability of trimeric OmpF porin: The contributions of the latching loop L2. *Biochemistry* **37**, 15663–15670.
- Popot, J., and Engelman, D. (1990). Membrane protein folding and oligomerization: The two-stage model. *Biochemistry* **29**, 4031–4037.
- Popot, J., and Engelman, D. (2000). Helical membrane protein folding, stability, and evolution. *Annu. Rev. Biochem.* **69**, 881–922.
- Rapoport, T. A. (2007). Protein translocation across the eukaryotic endoplasmic reticulum and bacterial plasma membranes. *Nature* **450**, 663–669.
- Reddy, L., Jones, L., and Thomas, D. (1999). Depolymerization of phospholamban in the presence of calcium pump: A fluorescence energy transfer study. *Biochemistry* **38**, 3954–3962.
- Remy, I., and Michnick, S. W. (1999). Clonal selection and in vivo quantitation of protein interactions with protein-fragment complementation assays. *Proc. Natl. Acad. Sci. USA* **96**, 5394–5399.
- Renthal, R. (2006). An unfolding story of helical transmembrane proteins. *Biochemistry* **45**, 14559–14566.
- Rostovtseva, T. K., Kazemi, N., Weinrich, M., and Bezrukov, S. M. (2006). Voltage gating of VDAC is regulated by nonlamellar lipids of mitochondrial membranes. *J. Biol. Chem.* **281**, 37496–37506.
- Russ, W., and Engelman, D. (1999). TOXCAT: A measure of transmembrane helix association in a biological membrane. *Proc. Natl. Acad. Sci. USA* **96**, 863–868.
- Schneider, D., and Engelman, D. M. (2003). GALLEX, a measurement of heterologous association of transmembrane helices in a biological membrane. *J. Biol. Chem.* **278**, 3105–3111. Epub 2002 November 21.
- Sehgal, P., Mogensen, J., and Otzen, D. (2005). Using micellar mole fractions to assess membrane protein stability in mixed micelles. *Biochim. Biophys. Acta* **1716**, 59–68.
- Sehgal, P., and Otzen, D. (2006). Thermodynamics of unfolding of an integral membrane protein in mixed micelles. *Protein Sci.* **15**, 890–899.

- Senes, A., Chadi, D. C., Law, P. B., Walters, R. F., Nanda, V., and Degrado, W. F. (2007). E(z), a depth-dependent potential for assessing the energies of insertion of amino acid side-chains into membranes: Derivation and applications to determining the orientation of transmembrane and interfacial helices. *J. Mol. Biol.* **366**, 436–448.
- Serrano, L., Bycroft, M., and Fersht, A. R. (1991). Aromatic-aromatic interactions and protein stability. Investigation by double-mutant cycles. *J. Mol. Biol.* **218**, 465–475.
- Stanley, A., and Fleming, K. (2007). The role of a hydrogen bonding network in the transmembrane beta-barrel OMPLA. *J. Mol. Biol.* **370**, 912–924.
- Stanley, A., and Fleming, K. (2008). The process of folding proteins into membranes: Challenges and progress. *Arch. Biochem. Biophys.* **469**, 46–66.
- Surrey, T., and Jahnig, F. (1992). Refolding and oriented insertion of a membrane protein into a lipid bilayer. *Proc. Natl. Acad. Sci. USA* **89**, 7457–7461.
- Tamm, L. K., Arora, A., and Kleinschmidt, J. H. (2001). Structure and assembly of beta-barrel membrane proteins. *J. Biol. Chem.* **276**, 32399–32402. Epub 2001 June 29.
- Tanford, C. (1979). Interfacial free energy and the hydrophobic effect. *Proc. Natl. Acad. Sci. USA* **76**, 4175–4176.
- Tanford, C., Nozaki, Y., Reynolds, J., and Makino, S. (1974). Molecular characterization of proteins in detergent solutions. *Biochemistry* **13**, 2369–2376.
- Ulmschneider, M. B., Sansom, M. S., and Di Nola, A. (2005). Properties of integral membrane protein structures: Derivation of an implicit membrane potential. *Proteins* **59**, 252–265.
- Wimley, W. C. (2002). Toward genomic identification of beta-barrel membrane proteins: Composition and architecture of known structures. *Protein Sci.* **11**, 301–312.
- Wimley, W. C., and White, S. H. (1996). Experimentally determined hydrophobicity scale for proteins at membrane interfaces. *Nat. Struct. Biol.* **3**, 842–848.
- Wu, T., Malinverni, J., Ruiz, N., Kim, S., Silhavy, T. J., and Kahne, D. (2005). Identification of a multicomponent complex required for outer membrane biogenesis in *Escherichia coli*. *Cell* **121**, 235–245.
- You, M., Li, E., Wimley, W., and Hristova, K. (2005). Forster resonance energy transfer in liposomes: Measurements of transmembrane helix dimerization in the native bilayer environment. *Anal. Biochem.* **340**, 154–164.